

## Supporting Information

for

### Introducing a Nested Multimedia Fate and Transport Model for Organic Contaminants (NEM)

Knut Breivik <sup>1,2,\*</sup>, Sabine Eckhardt <sup>1</sup>, Michael S. McLachlan <sup>3</sup> and Frank Wania <sup>4</sup>

<sup>1</sup> Norwegian Institute for Air Research, Box 100, NO-2027 Kjeller, Norway

<sup>2</sup> Department of Chemistry, University of Oslo, Box 1033, NO-0315 Oslo, Norway

<sup>3</sup> Department of Environmental Science and Analytical Chemistry (ACES), Stockholm University, SE-106 91 Stockholm, Sweden

<sup>4</sup> Department of Physical and Environmental Sciences, University of Toronto Scarborough, 1265 Military Trail, Toronto, Ontario, Canada M1C 1A4

*Corresponding author and address:*

Knut Breivik, Norwegian Institute for Air Research, Box 100, NO-2027 Kjeller, Norway  
kbr@nilu.no, Phone: +47 63898000, Fax: +47 63898050

Total 20 pages: Tables S1-S2 and Figures S1-S16.

Table S1: Stations, station coordinates, years covered (ebas.nilu.no) and selected references \*).

Station	Coordinates	Years covered	References (selected)
Andøya (Norway)	69°16'N, 16°00'E	2010-2017	1
Birkenes (Norway)	58°23'N, 08°15'E	2004-2019	2, 3
Košetice (Czech Republic)	49°34'N, 15°04'E	1999-2014	4, 5
Pallas (Finland)	68°00'N, 24°15'E	1996-2018	6
Aspvreten (Finland)	58°48'N, 17°23'E	1995-2018	7
Rörvik (Sweden)	57°25'N, 11°56'E	1994-2001	
Råö (Sweden)	57°23'N, 11°54'E	2002-2018	6
Stórhöfði (Iceland)	63°24'N, 20°17'W	1995-2018	8
Zeppelin ( Spitsbergen)	78°54'N, 11°53'E	1998-2019	9

\*) Data from four additional stations with more limited time-series were available from ebas.nilu.no. These stations are High Muffles in Great Britain (54°20'N, 00°48'W: 2004-2008), Schauinsland (47°54'N, 07°54'E: 2007-2010), Westerland (54°55'N, 08°18'E: 2007-2010) and Zingst in Germany (54°26'N, 12°43'E: 2009-2010). These data were only included for the initial model evaluation for the sake of completeness (Figure S5).

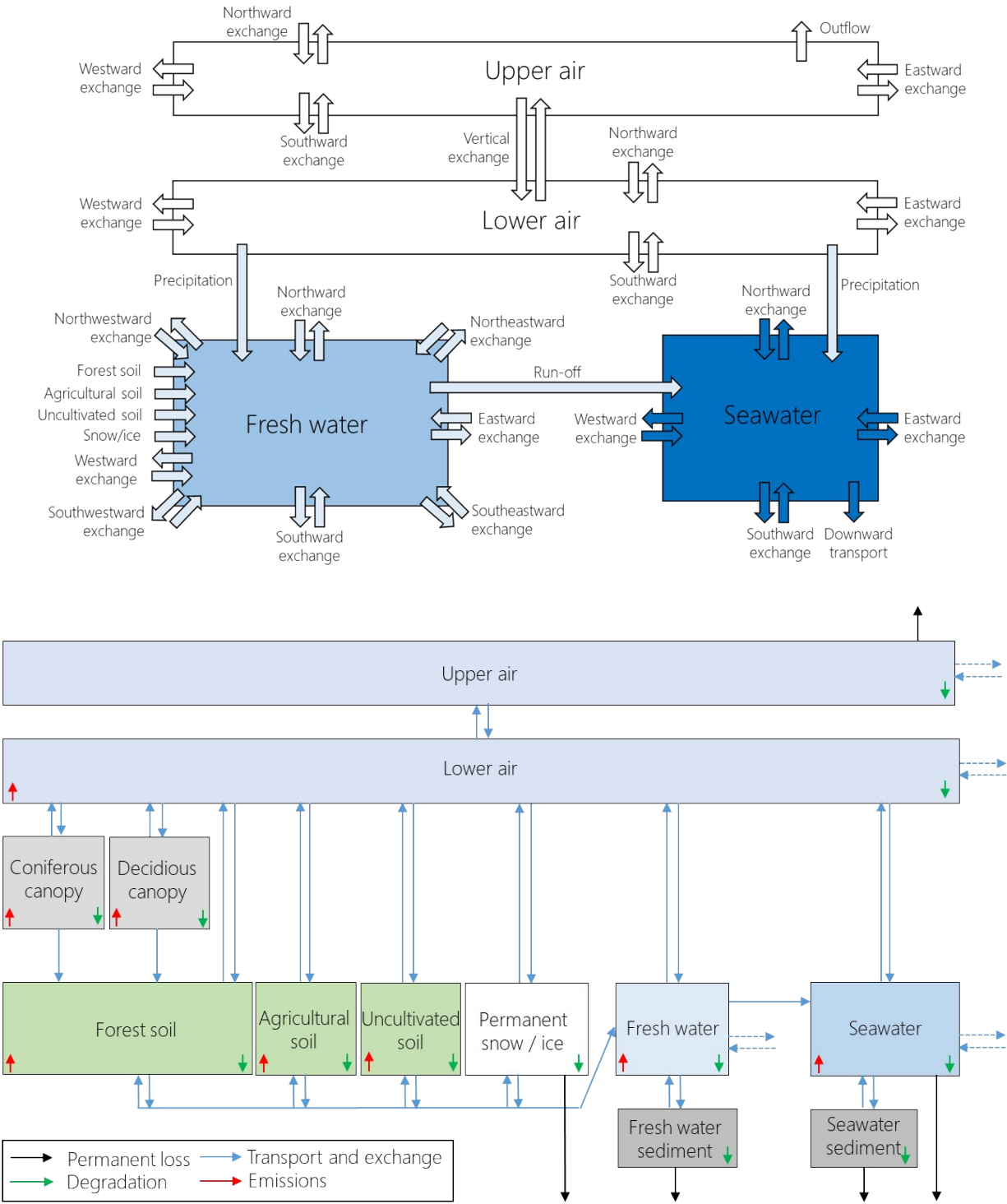


Figure S1: Transport of air, fresh water and seawater in the air-fresh water-seawater system (top) and chemical transport and fate processes included for each compartment (bottom) that are included within each grid cell.

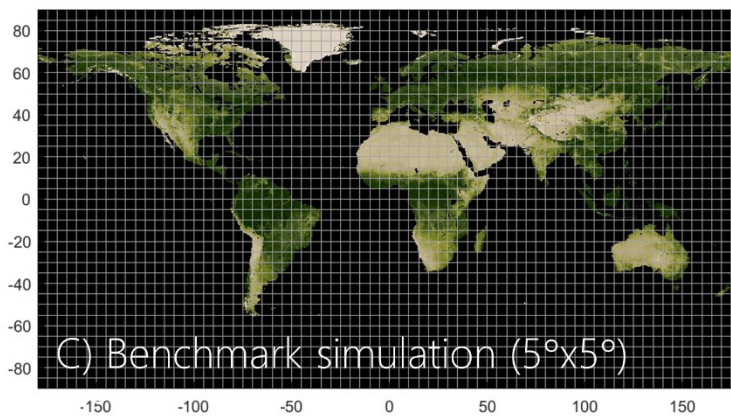
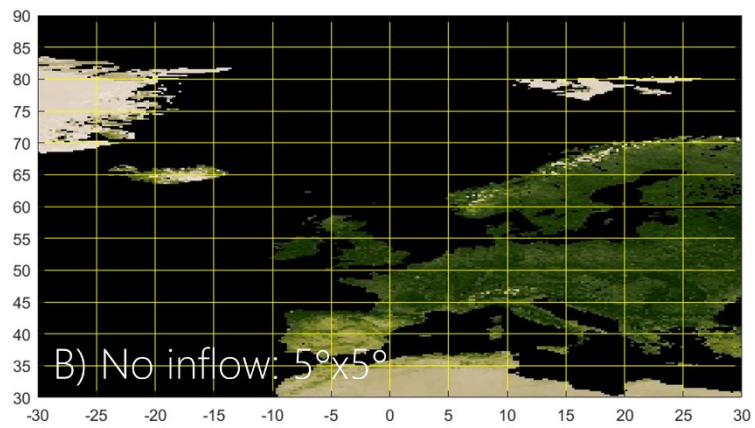
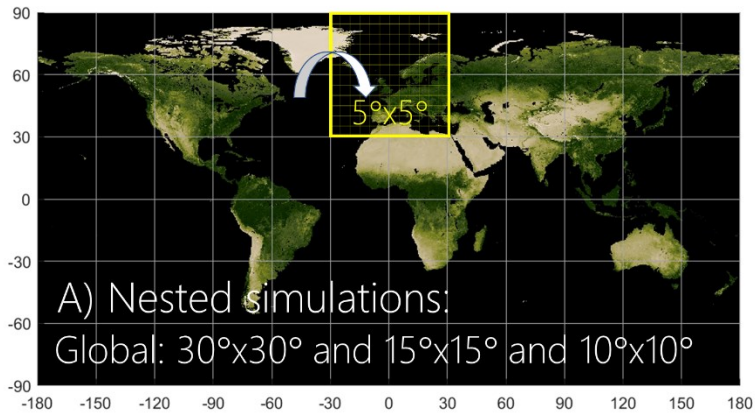


Figure S2: Illustration of the modelling approach used to explore the impact of the spatial resolution of the external global domain on the predicted concentrations of PCB-153 within a nested European region (90°N, 30°W to 30°N, 30°E) with a 5°x5° resolution.

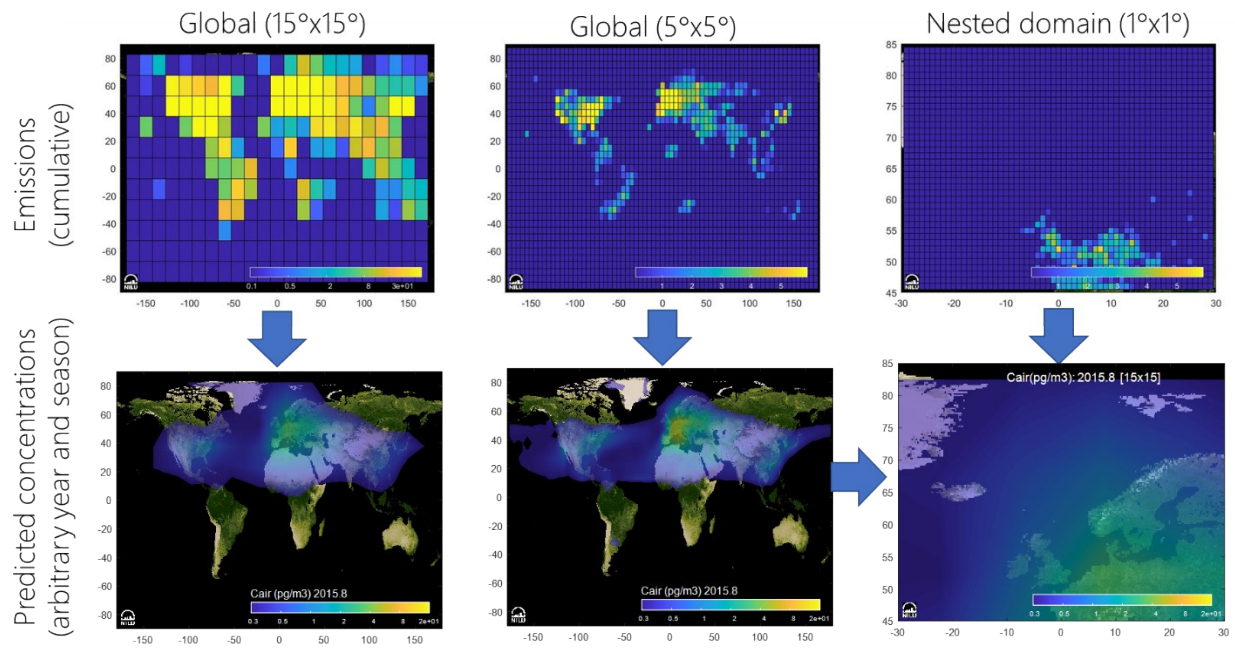


Figure S3: Illustration of the modelling approach used for the model evaluation and application for the Northern European domain (85°N, 30°W to 45°N, 30°E).

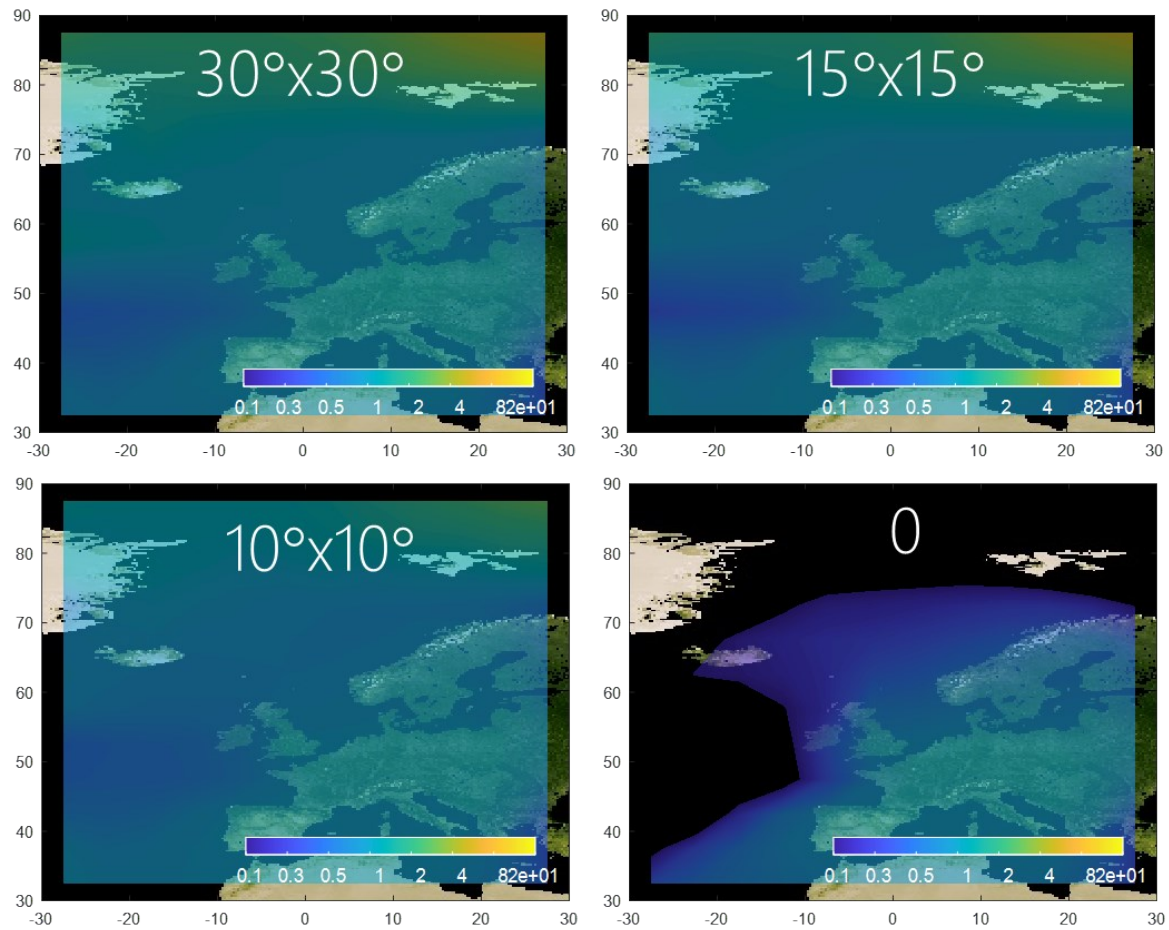


Figure S4: Impact of variable resolutions outside a nested domain on predictions within a nested domain (90°N, 30°W to 30°N, 30°E). The maps show the predicted concentration in air from three nested simulations at 5°x5°, relying on outputs from global simulations (30°x30°; 15°x15° and 10°x10°) as input, divided by the predicted concentrations from the global reference simulation at 5°x5° during late summer, 2015. The lower panel to the right shows the results from the scenario without any inflow of PCB-153 into the nested domain.



Figure S5: Observed long-term trends of PCB-153 in air for four additional monitoring sites versus model predictions based on different spatial resolutions (15°x15°, 5°x5°, 1°x1°).

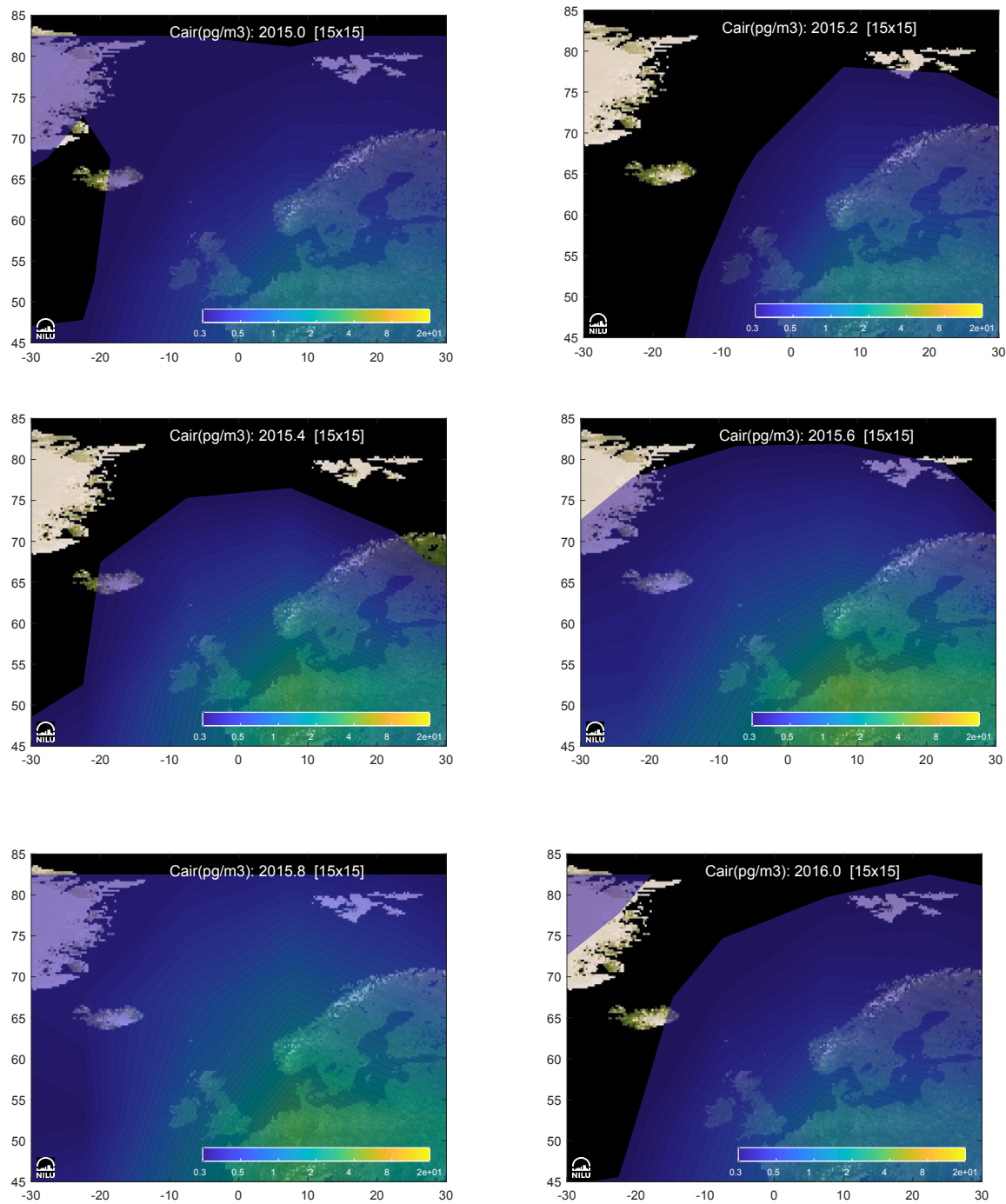


Figure S6: Predicted concentrations of PCB-153 in air during 2015 at 15°x15°.



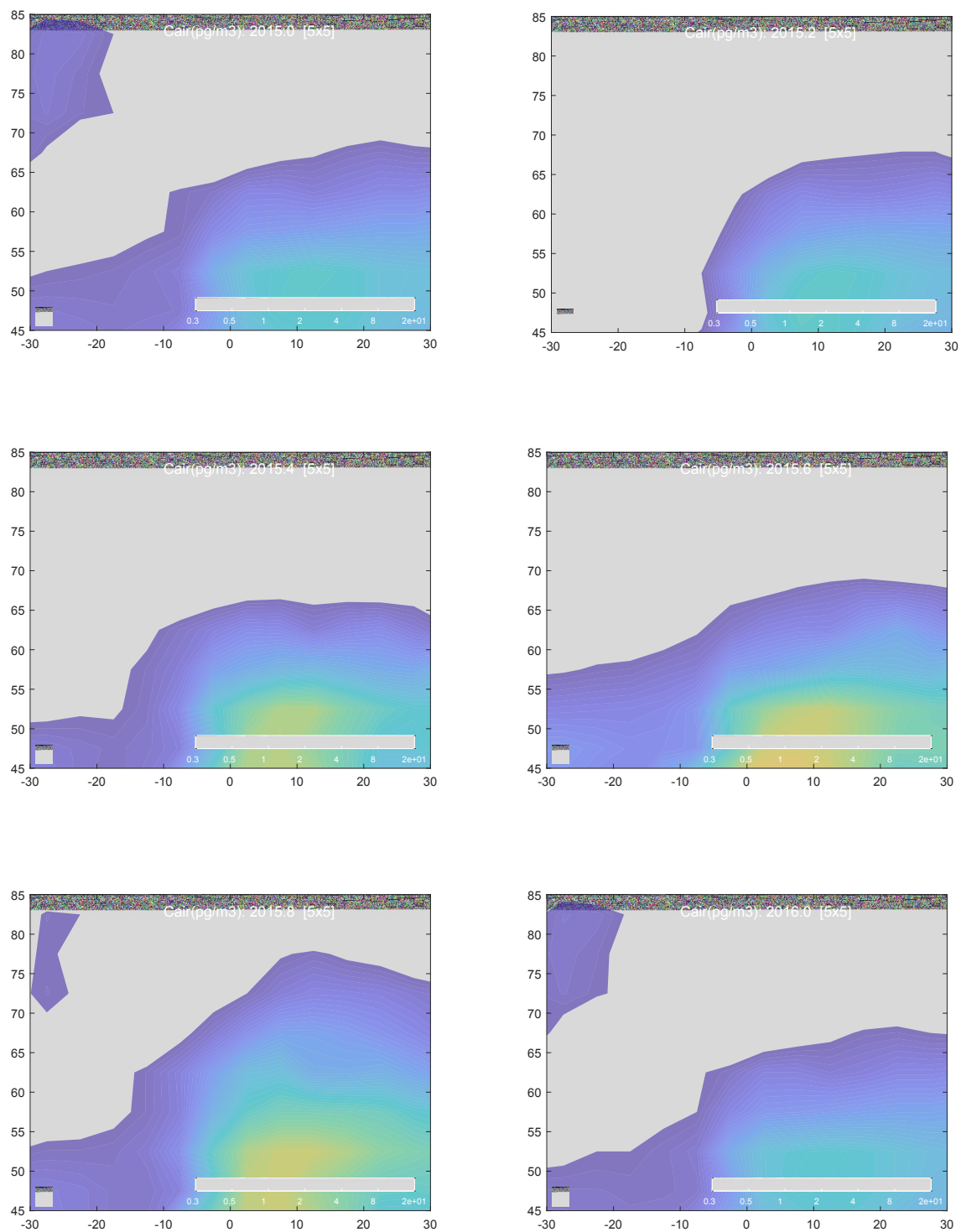


Figure S7: Predicted concentrations of PCB-153 in air during 2015 at 5°x5°.

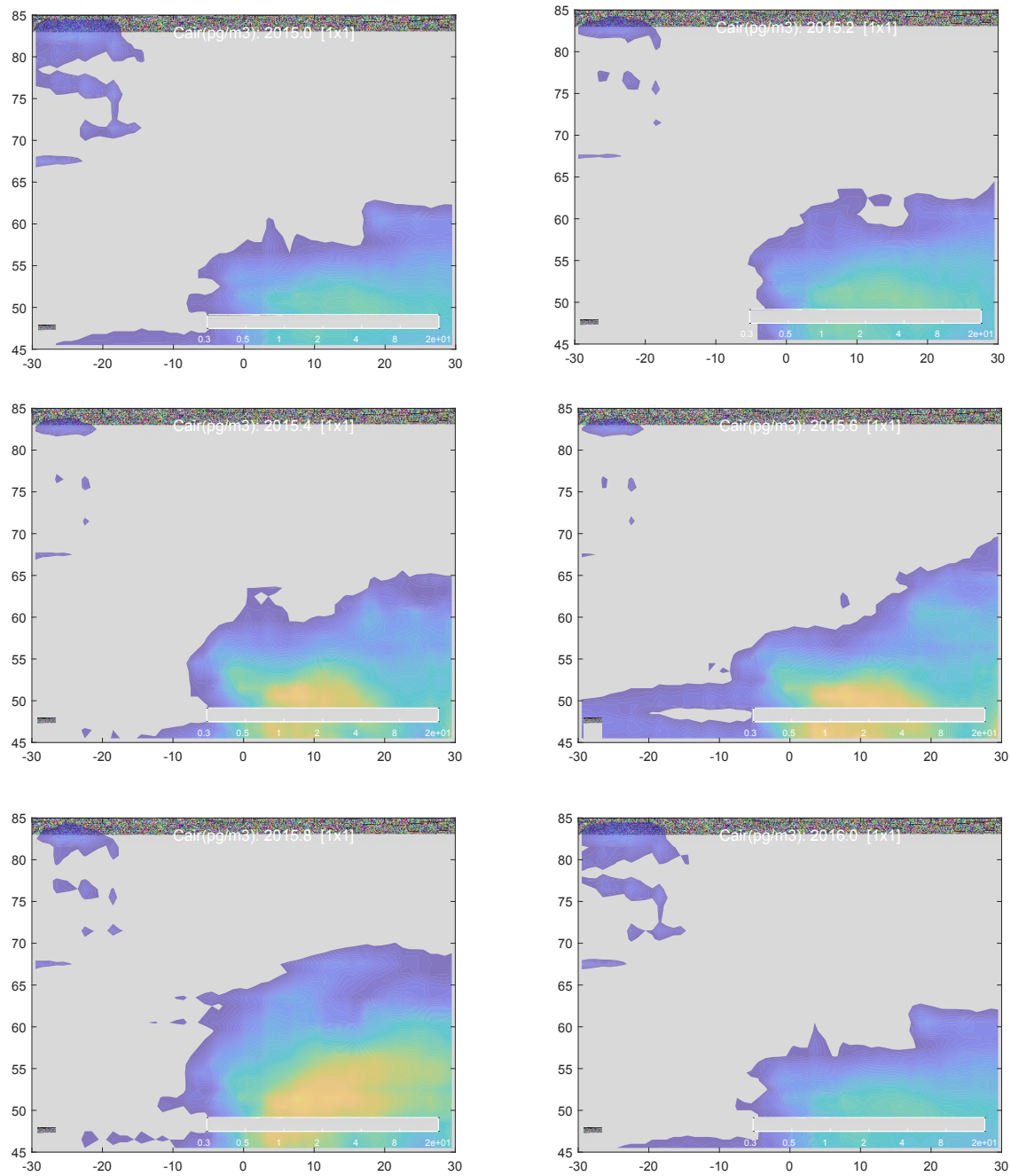
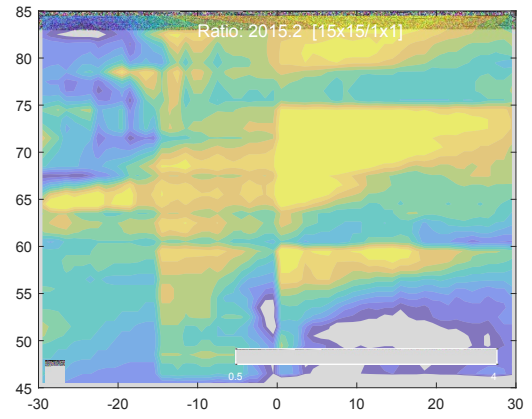
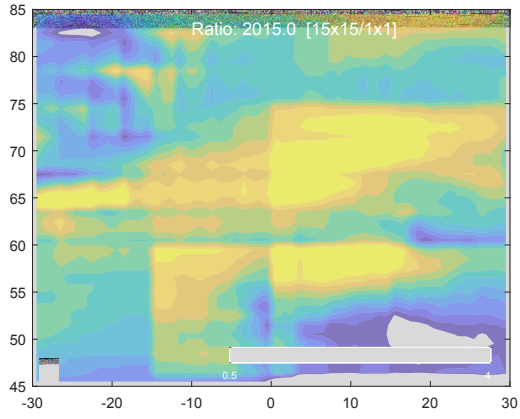


Figure S8: Predicted concentrations of PCB-153 in air during 2015 at 1°x1°.



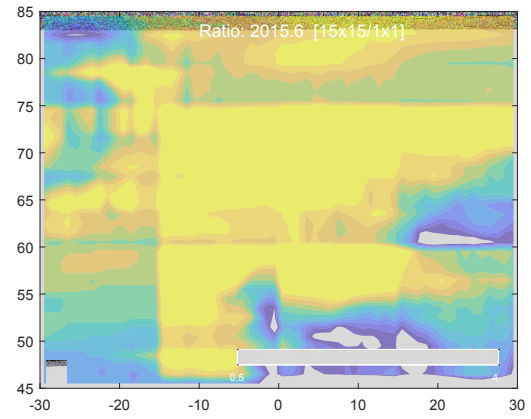
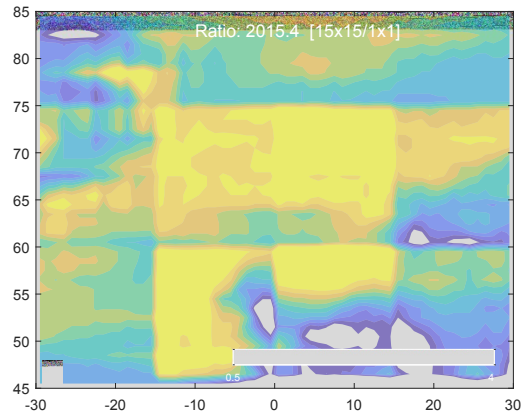
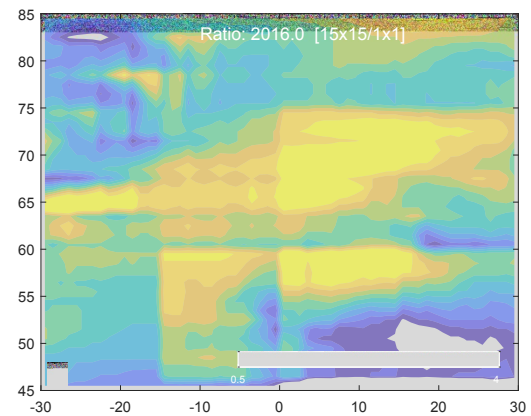
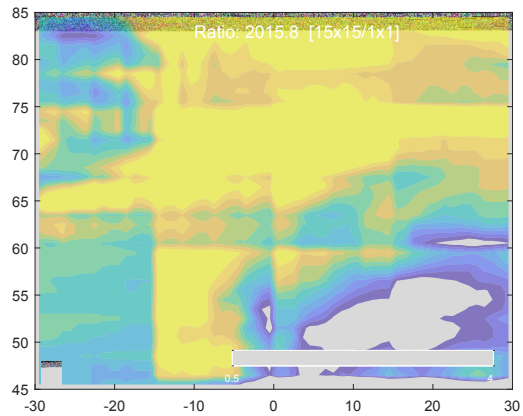


Figure S9: Predicted concentrations of PCB-153 in air during 2015 at 15°x15°, divided by predictions obtained at 1°x1°.



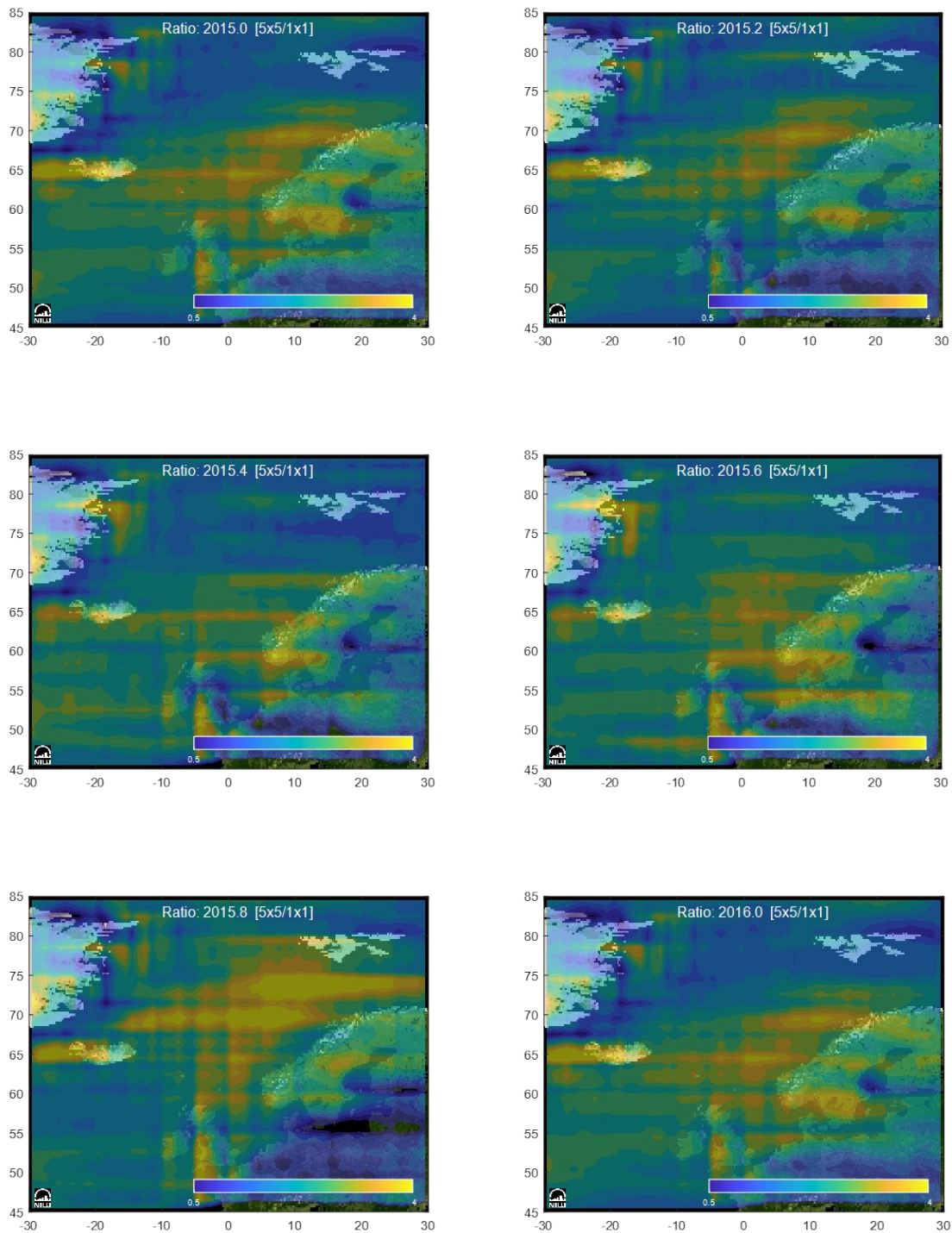


Figure S10: Predicted concentrations of PCB-153 in air during 2015 at 5°x5°, divided by predictions obtained at 1°x1°.

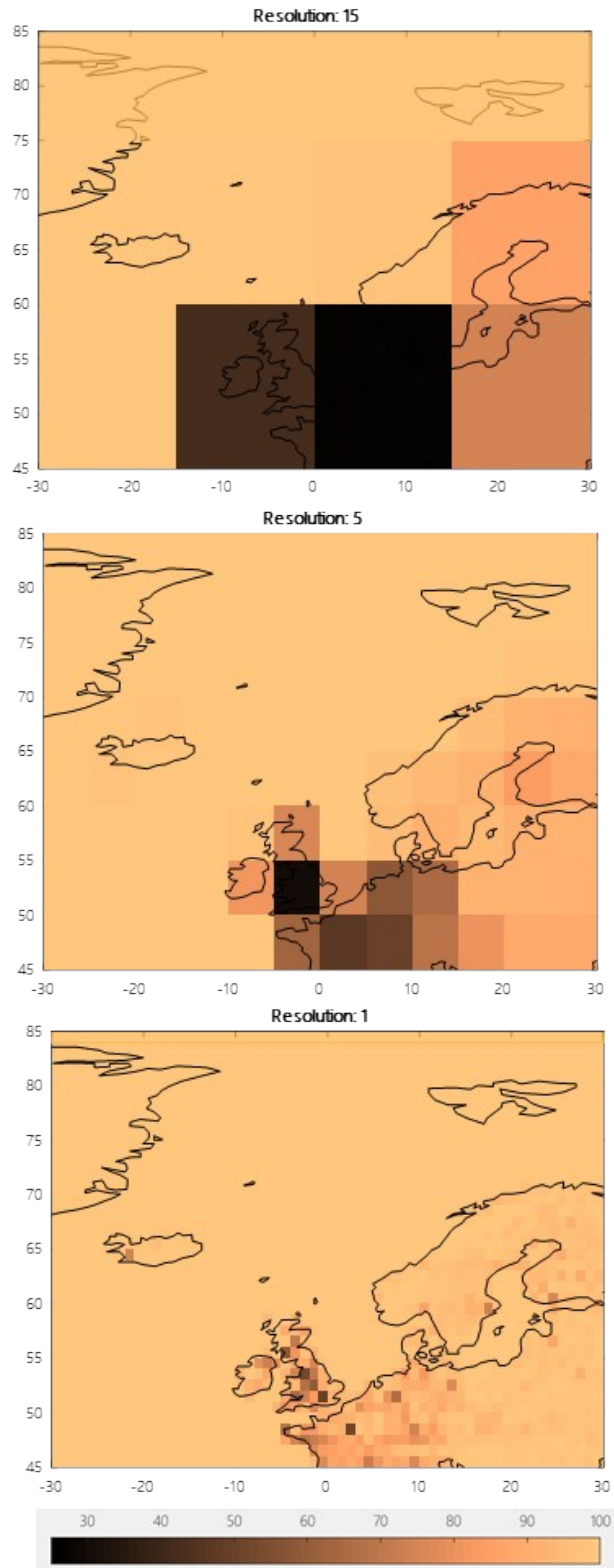


Figure S11: Relative significance of atmospheric inflow to the sum of atmospheric inflow plus emissions, simulated using three different spatial resolutions, 1930-2020 ( $15^\circ \times 15^\circ$ ,  $5^\circ \times 5^\circ$ ,  $1^\circ \times 1^\circ$ ).

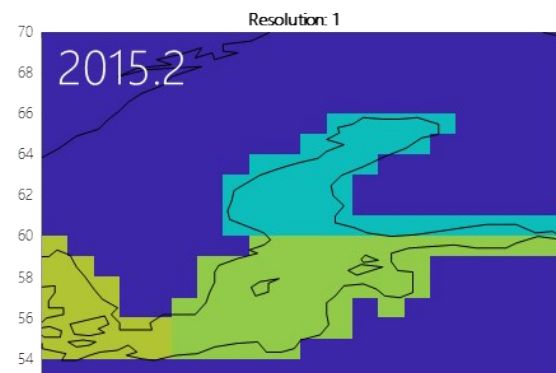
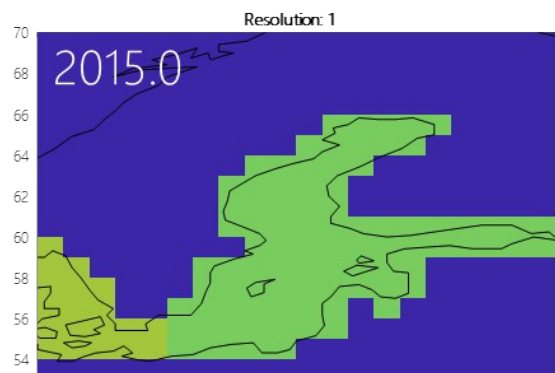
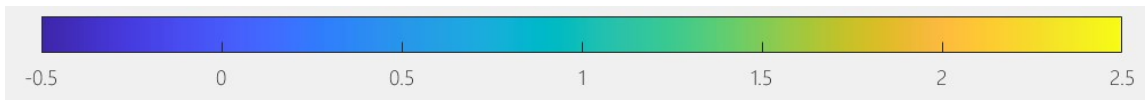


Figure S12: Predicted atmospheric deposition of PCB-153 to the Baltic Sea during 2015 at 15°x15° in ng m<sup>-2</sup> h<sup>-1</sup> (log<sub>10</sub>). The Baltic Sea is defined at a 1°x1° degree resolution.



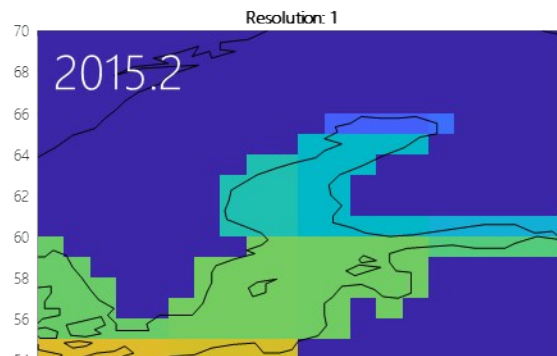
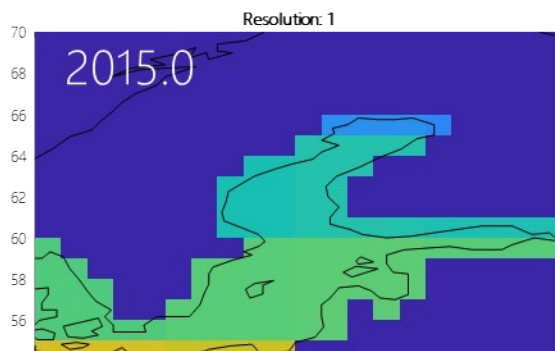
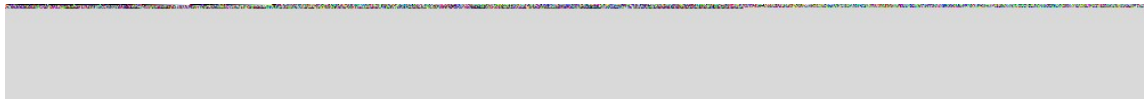


Figure S13: Predicted atmospheric deposition of PCB-153 to the Baltic Sea during 2015 at 5°x5° in  $\text{ng m}^{-2} \text{h}^{-1}$  ( $\log_{10}$ ). The Baltic Sea is defined at a 1°x1° degree resolution.

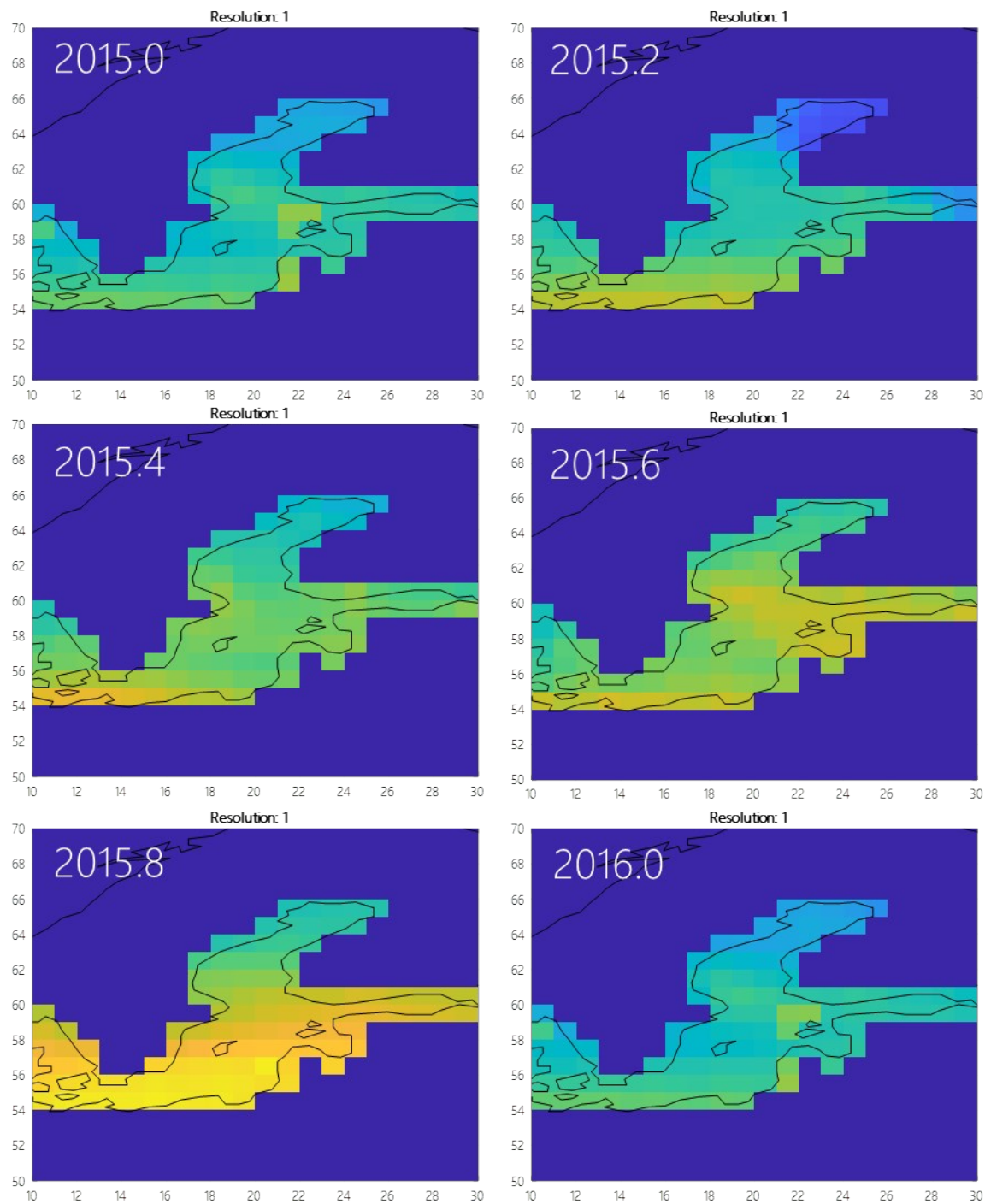


Figure S14: Predicted atmospheric deposition of PCB-153 to the Baltic Sea during 2015 at  $1^\circ \times 1^\circ$  in  $\text{ng m}^{-2} \text{h}^{-1}$  ( $\log_{10}$ ). The Baltic Sea is defined at a  $1^\circ \times 1^\circ$  degree resolution.

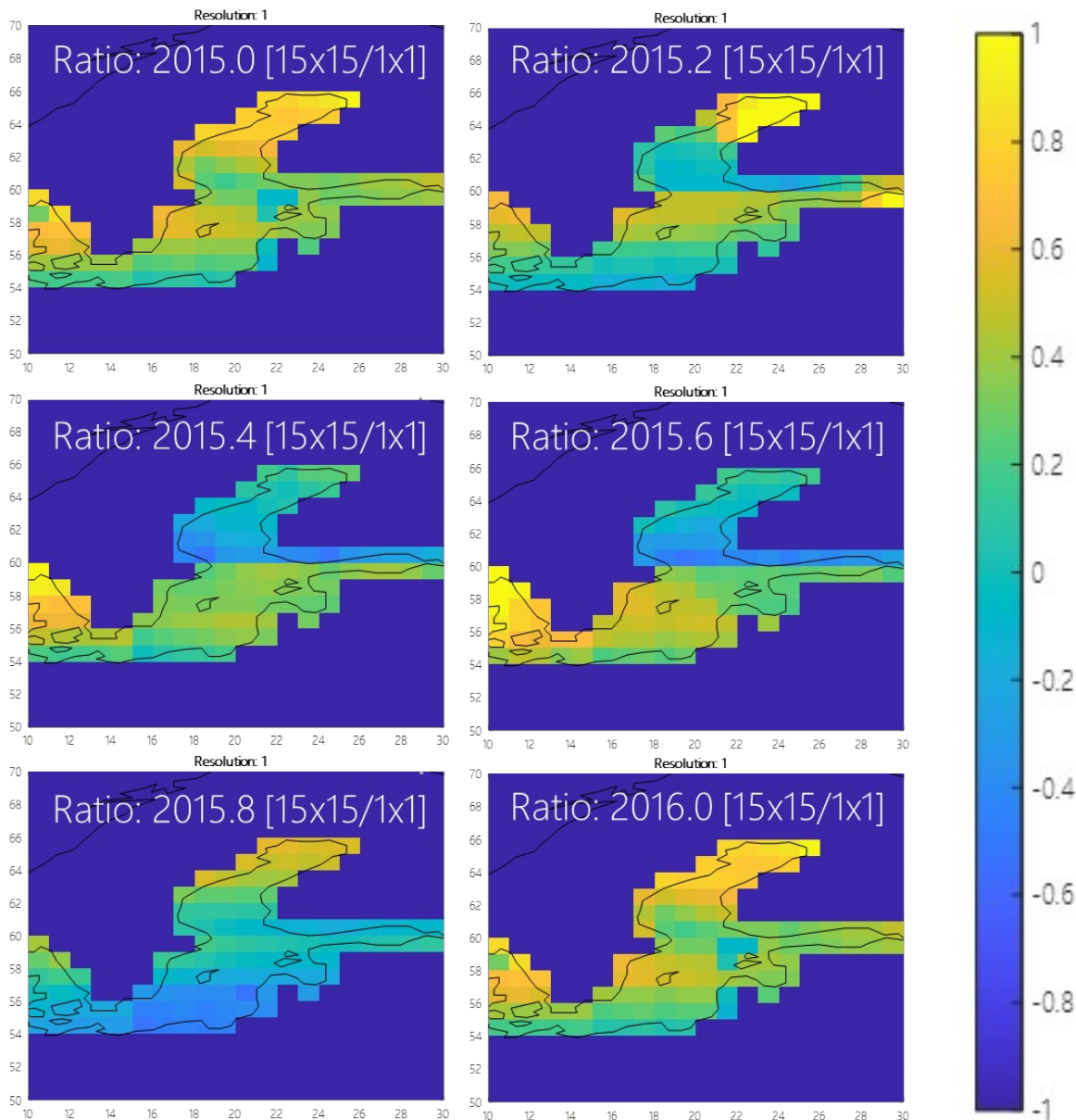


Figure S15: Logarithm of the ratio of 2015 atmospheric deposition flux of PCB-153 to the Baltic Sea predicted with NEM at a resolution of  $15^\circ \times 15^\circ$  and  $1^\circ \times 1^\circ$ . A value of 0 indicates the same predicted deposition, positive values (yellow) indicate higher deposition at coarser resolution and negative values (blue) designate lower deposition at coarser resolution. A value of 1

corresponds to differences in deposition by one order of magnitude. The Baltic Sea is defined at a  $1^\circ \times 1^\circ$  degree resolution.

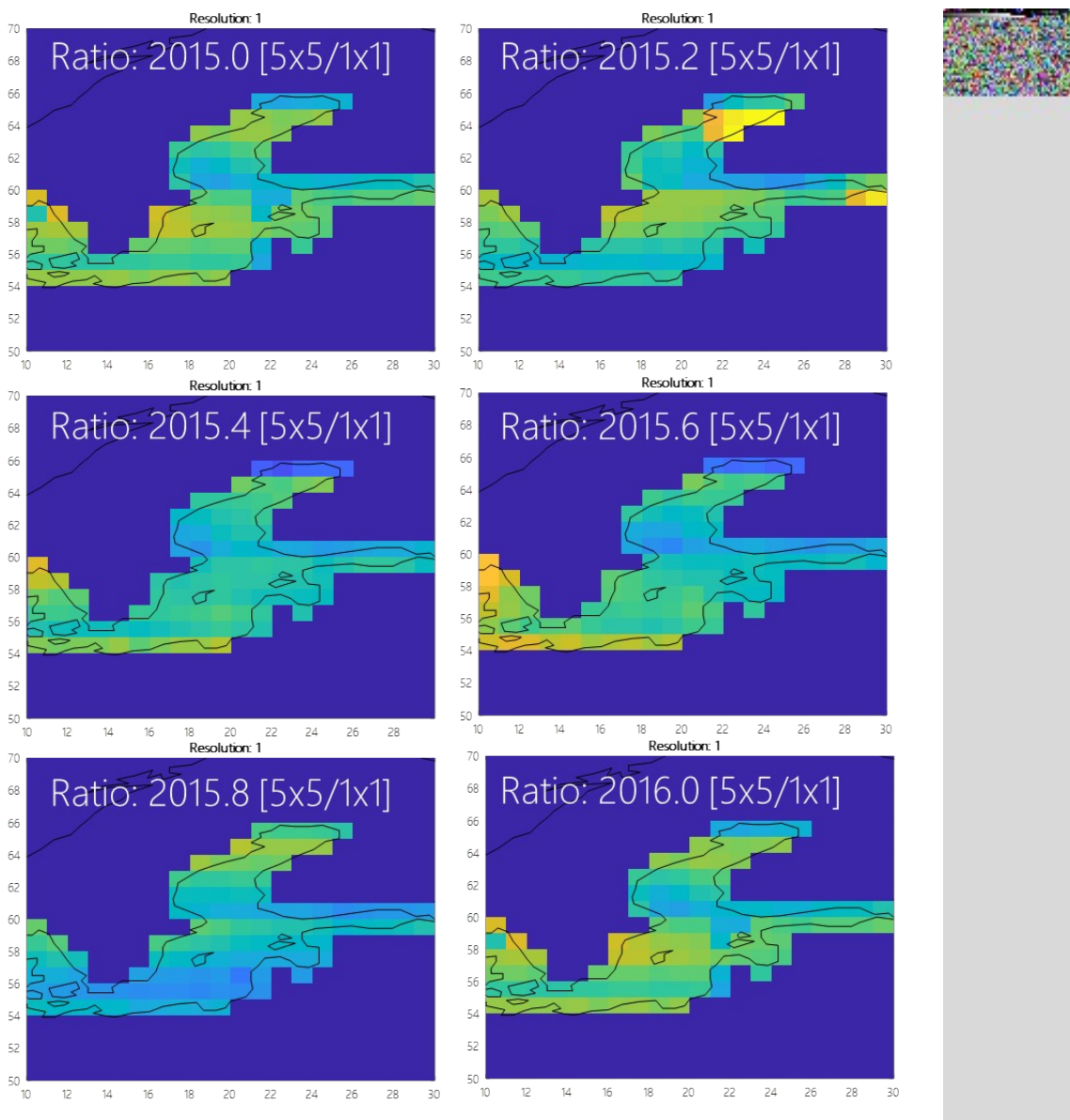


Figure S16: Logarithm of the ratio of 2015 atmospheric deposition flux of PCB-153 to the Baltic Sea predicted with NEM at a resolution of  $5^\circ \times 5^\circ$  and  $1^\circ \times 1^\circ$ . A value of 0 indicates the same predicted deposition, positive values (yellow) indicate higher deposition at coarser resolution and negative values (blue) designate lower deposition at coarser resolution. A value of 1 corresponds to differences in deposition by one order of magnitude. The Baltic Sea is defined at a  $1^\circ \times 1^\circ$  degree resolution.

Table S2: Seasonal atmospheric deposition flux of PCB-153 to the Baltic Sea predicted with NEM at a resolution of 15°x15°, 5°x5° and 1°x1° (Kg/Year). The Baltic Sea is defined at a 1°x1° degree resolution, and the three different basins at 15°x15° are defined as in the main text and as illustrated in Figure S13.

<b>Time</b>	<b>Resolution</b>	<b>Kattegat/ Skagerrak</b>	<b>Baltic Proper</b>	<b>Bothnian Sea</b>	<b>Baltic Sea (Total)</b>
<b>2015.0</b>	15°x15°	3.2	6.5	3.5	13.2
	5°x5°	2.7	5.7	1.2	9.6
	1°x1°	1.4	3.5	1.2	6.0
<b>2015.2</b>	15°x15°	3.6	7.8	1.1	12.6
	5°x5°	3.2	6.7	1.0	10.9
	1°x1°	2.4	4.9	0.9	8.2
<b>2015.4</b>	15°x15°	9.0	13.3	1.3	23.7
	5°x5°	6.3	8.7	1.7	16.8
	1°x1°	3.4	6.6	2.0	12.0
<b>2015.6</b>	15°x15°	11.0	20.5	2.2	33.6
	5°x5°	7.3	11.7	2.7	21.7
	1°x1°	2.5	8.8	3.7	15.0
<b>2015.8</b>	15°x15°	9.0	16.6	4.9	30.5
	5°x5°	9.4	18.9	3.5	31.8
	1°x1°	12.2	29.5	3.5	45.2
<b>2016.0</b>	15°x15°	3.0	6.1	3.3	12.5
	5°x5°	2.6	5.3	1.1	9.0
	1°x1°	1.3	3.3	1.1	5.6

## References

1. Wong, F.; Shoeib, M.; Katsoyiannis, A.; Eckhardt, S.; Stohl, A.; Bohlin-Nizzetto, P.; Li, H.; Fellin, P.; Su, Y.; Hung, H., Assessing temporal trends and source regions of per- and polyfluoroalkyl substances (PFASs) in air under the Arctic Monitoring and Assessment Programme (AMAP). *Atmospheric Environment* **2018**, *172*, 65-73.
2. Eckhardt, S.; Breivik, K.; Li, Y. F.; Manø, S.; Stohl, A., Source regions of some persistent organic pollutants measured in the atmosphere at Birkenes, Norway. *Atmospheric Chemistry and Physics* **2009**, *9*, (17), 6597-6610.
3. Halse, A. K.; Eckhardt, S.; Schlabach, M.; Stohl, A.; Breivik, K., Forecasting long-range atmospheric transport episodes of polychlorinated biphenyls using FLEXPART. *Atmospheric Environment* **2013**, *71*, 335-339.
4. Dvorska, A.; Lammel, G.; Klanova, J.; Holoubek, I., Kosetice, Czech Republic - ten years of air pollution monitoring and four years of evaluating the origin of persistent organic pollutants. *Environ. Pollut.* **2008**, *156*, (2), 403-408.
5. Dvorska, A.; Lammel, G.; Holoubek, I., Recent trends of persistent organic pollutants in air in central Europe - Air monitoring in combination with air mass trajectory statistics as a tool to study the effectivity of regional chemical policy. *Atmospheric Environment* **2009**, *43*, (6), 1280-1287.
6. Anttila, P.; Brorstrom-Lunden, E.; Hansson, K.; Hakola, H.; Vestenius, M., Assessment of the spatial and temporal distribution of persistent organic pollutants (POPs) in the Nordic atmosphere. *Atmospheric Environment* **2016**, *140*, 22-33.
7. Sellstrom, U.; Egeback, A. L.; McLachlan, M. S., Identifying source regions for the atmospheric input of PCDD/Fs to the Baltic Sea. *Atmospheric Environment* **2009**, *43*, (10), 1730-1736.
8. Hung, H.; Katsoyiannis, A. A.; Brorström-Lundén, E.; Olafsdottir, K.; Aas, W.; Breivik, K.; Bohlin-Nizzetto, P.; Sigurdsson, A.; Hakola, H.; Bossi, R.; Skov, H.; Sverko, E.; Barresi, E.; Fellin, P.; Wilson, S., Temporal trends of Persistent Organic Pollutants (POPs) in arctic air: 20 years of monitoring under the Arctic Monitoring and Assessment Programme (AMAP). *Environ. Pollut.* **2016**, *217*, 52-61.
9. Eckhardt, S.; Breivik, K.; Manø, S.; Stohl, A., Record high peaks in PCB concentrations in the Arctic atmosphere due to long-range transport of biomass burning emissions. *Atmospheric Chemistry and Physics* **2007**, *7*, (17), 4527-4536.